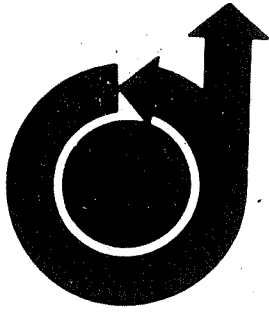


R73-45



TECHNICAL LIBRARY
U. S. ARMY
NATICK LABORATORIES
NATICK, MASS. 01760

**AIAA Paper
No. 73-462**

ANALYSIS OF VARIOUS AUTOMATIC HOMING TECHNIQUES
FOR GLIDING AIRDROP SYSTEMS WITH COMPARATIVE
PERFORMANCE IN ADVERSE WINDS

by
THOMAS F. GOODRICK, ALLAN PEARSON,
and
A. L. MURPHY, JR.
U.S. Army Natick Laboratories
Natick, Massachusetts

AIAA 4th Aerodynamic Deceleration Systems Conference

PALM SPRINGS, CALIFORNIA / MAY 21-23, 1973

First publication rights reserved by American Institute of Aeronautics and Astronautics,
1290 Avenue of the Americas, New York, N. Y. 10019. Abstracts may be published without
permission if credit is given to author and to AIAA. (Price: AIAA Member \$1.50. Nonmember \$2.00).

Note: This paper available at AIAA New York office for six months;
thereafter, photoprint copies are available at photocopy prices from
AIAA Library, 750 3rd Avenue, New York, New York 10017

ANALYSIS OF VARIOUS AUTOMATIC HOMING TECHNIQUES FOR GLIDING
AIRDROP SYSTEMS WITH COMPARATIVE PERFORMANCE IN ADVERSE WINDS

Thomas F. Goodrick, Allan Pearson* and A.L. Murphy, Jr.**
Airdrop Engineering Laboratory
US Army Natick Laboratories
Natick, Massachusetts

Abstract

The US Army Natick Laboratories is conducting extensive theoretical analyses of automatic homing techniques for gliding airdrop systems for the purpose of optimizing landing accuracy and groundspeed. The analyses presented in this paper include application of optimal control theory, general analysis of the basic equations of motion and analysis of the comparative performance of several homing methods in adverse winds using computer simulation. The results may serve as the basis for design of guidance hardware according to specific user needs for accuracy in certain operational environments. The analytical techniques may stimulate interest in further studies since solution of the problem for a general wind environment is by no means complete. In this paper the problem is limited to unperturbed steady aerodynamic flight with steering at bank angles less than thirty degrees in either constant wind or varying wind having accelerations of less than two ft/sec/sec. Optimal control theory provides quantitative consideration of key parametric relations although exact solution to the equations requires sophisticated computation not practical for incorporation into guidance hardware. Analysis of the basic equations of motion in a less restricted sense yields closed-form solutions assuming constant wind. These include radial homing and a computed homing method which requires complete sensory input data. The computed homing method gives perfect accuracy with minimum landing speed in wind of any magnitude. Results of the simulated performance in adversely varying winds show the more sophisticated methods offer only slightly improved accuracy than simple radial homing.

Symbols

h Instantaneous height
P Magnitude of position vector in wind coordinates
p Magnitude of position vector in inertial coordinates

*Currently Professor of Engineering, Division of Engineering, Brown University. Visiting Scientist at US Army Natick Laboratories from June through August 1972.

**Member, AIAA

r Radius of Turn
T Total time to ground
t Instantaneous elapsed time
u Horizontal airspeed component
v Rate of descent
w Wind speed
X,Y Wind-fixed coordinates
x,y Inertial coordinates
 β Angle between position vector and horizontal airspeed vector
 θ Polar angle of position vector
 ϕ Bank angle (angle between resultant aerodynamic force vector and vertical axis)
 ψ Polar angle of horizontal airspeed vector ($\psi = \theta + \beta$)
 ω Polar angle of wind vector (inertial)

1.0 Introduction

The US Army Natick Laboratories is conducting various studies of the potential use of high performance gliding airdrop systems. Since any application of gliding airdrop systems to cargo delivery necessitates incorporation of a guidance subsystem, considerable effort is being expended in studying the aspects of homing control peculiar to low speed gliders in the wind environment. Although actual homing systems have been tested by other agencies, the theoretical aspects of various homing methods have not been studied in significant detail. Thus, before initiating any hardware development, this Laboratory has undertaken theoretical studies of homing methods in order to ascertain their salient characteristics. The work presented in this paper summarizes this effort to date. While the study has indicated the merits and salient features of several concepts, it will become clear to the reader that much opportunity remains for improvement in capabilities within a variable-wind environment.

The basic problem as considered in this paper is to formulate principles by which a steadily moving point can be guided over the ground so that it arrives at a predetermined target point after a fixed time interval. The vertical velocity of the point is assumed constant. The lateral motion is determined by the constant airspeed, the radius of turn with respect to air and by the displacement caused by wind. The sole means of guidance control is assumed to be variation of the radius of turn (or the related turn rate, $\dot{\psi}$). The radius of turn varies inversely with the tangent of the bank angle. The bank angle is varied by canopy deflection actuated by servo motors. Although varying winds are

employed, the variation is assumed to be insufficient to disturb the steady aerodynamic motion so that the sole effect of the wind is a displacement relative to the ground.

This paper presents three different approaches to the problem. The first approach applies the mathematics of optimal control theory with a system of equations formulated to optimize accuracy, landing speed, and turn rate. The second approach involves solution of the basic equations of motion with several simple steering functions. The third approach involves computer simulation of various feedback steering laws predicated on various amounts of sensory input data.

Although no specific consideration has been given to design requirements for guidance hardware, most control methods presented in this paper are within the state-of-the-art in guidance technology. The most sophisticated method used in the final comparative performance study (Method D) would require a radio navigation system comparable to the aircraft omni-range with distance-measuring equipment (VOR/DME) although at substantially reduced power. The control logic could be performed by analog circuitry. The exact solution, however, of the optimal control equations would exceed the capacity of on-board computational equipment.

2.0 General Problem Definition

2.1 Steady Motion

The basic assumption to all analyses in this paper is that the rate of descent and the airspeed of a gliding airdrop system are steady and are not perturbed by changing wind velocity or by control actuation. Wind accelerations used in the study presented in Section 5.0 are always less than two ft/sec/sec. A longitudinal dynamic flight model of typical gliding systems shows that the effects of this acceleration are of second order and that the assumption of instantaneous response is reasonable. Control actuation for a turn causes both a change in steady state horizontal and vertical velocity components and a damped oscillation about the steady state values. These effects are neglected for the following reasons:

(1) Primarily only the vertical velocity is affected which changes the time of flight but not the homing characteristics.

(2) Where non-proportional (bang-bang) turn control is used as in Methods A, B and C, the motion consists mostly of steady oscillations between equal bank angles resulting in reasonably steady average velocity components.

(3) Where turn rate is continuously controlled, a maximum turn rate is fixed such that angle of bank does not exceed 30 degrees with turns at lower rates most of the time. The assumption of steady

motion greatly simplifies the analysis while neglecting effects which are only second order to the guidance problem.

2.2 Landing Constraints

The objective of a control method is to constrain the motion of a steadily moving point mass subject to wind drift so as to land near the intended target and to be heading into the wind. The two constraints are of equal importance since cargo would be lost either by landing too far from the target in most environments or by landing at a ground speed which is too high. The basic purpose for developing gliding airdrop systems is to land cargo on small unimproved drop zones. The difficulty of designing impact attenuation devices is significantly compounded at higher horizontal velocities due to uneven terrain and obstacles. Therefore, the landing speed should not exceed the landing speed for the no-wind case.

2.3 Equations of Motion

The basic equations of motion relative to inertial coordinates (Figure 1) are

$$\dot{p} = -u \cos\beta + W_x \cos\theta + W_y \sin\theta \quad (1)$$

$$p \dot{\theta} = -u \sin\beta - W_x \sin\theta + W_y \cos\theta \quad (2)$$

The equations governing turn control are

$$\dot{\gamma} = \theta + \beta + \pi \quad (3)$$

$$\dot{\gamma} = \dot{\theta} + \dot{\beta} \quad (4)$$

$$\dot{\gamma} = u/r \quad (5)$$

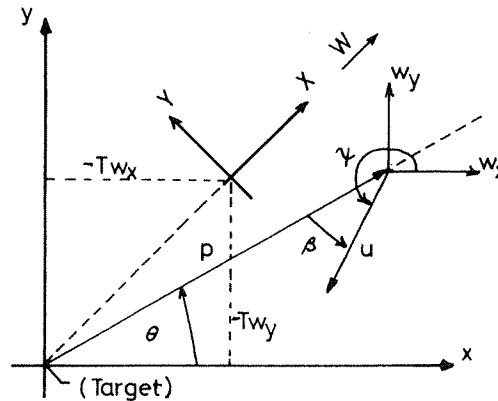


FIG1 GEOMETRIC RELATIONS

For iterative computation the following relations are used^{(1) (2)}

$$\Delta x = (r/u)(u_x \sin\Delta\gamma + a_{u_y}[\cos\Delta\gamma - 1]) \quad (6)$$

$$+ W_x \Delta t$$

$$\Delta y = (r/u)(u_y \sin\Delta\gamma - a_{u_x}[\cos\Delta\gamma - 1]) \quad (7)$$

$$+ W_y \Delta t$$

$$\Delta u_x = u_x(\cos\Delta\gamma - 1) - au_y \sin\Delta\gamma \quad (8)$$

$$\Delta u_y = u_y(\cos\Delta\gamma - 1) + au_x \sin\Delta\gamma \quad (9)$$

where

$$\Delta\gamma = \Delta t u / r \quad (10)$$

and

$$a = \left(\frac{xu_y - yu_x}{|xu_y - yu_x|} \right) \quad (11)$$

for "bang-bang" control (i.e., constant r). But $a = 1$ for proportional homing where the sign of r determines the direction of turn.

Transformation to a wind-fixed coordinate system is accomplished by the following relations which involve both translation $(x, y) \rightarrow (X_1, Y_1)$ and rotation $(X_1, Y_1) \rightarrow (X_2, Y_2)$:

$$X_1 = x + w_x h/v \quad (12)$$

$$Y_1 = y + w_y h/v \quad (13)$$

$$\omega = \arctan w_y/w_x \quad (14)$$

$$X_2 = X_1 \cos\omega + Y_1 \sin\omega \quad (15)$$

$$Y_2 = Y_1 \cos\omega - X_1 \sin\omega \quad (16)$$

$$\theta_2 = \arctan(Y_1/X_1) - \omega \quad (17)$$

$$\beta_2 = \arctan \left\{ \frac{Y_1 u_x - X_1 u_y}{-(X_1 u_x + Y_1 u_y)} \right\} \quad (18)$$

In a steady, uniform wind use of the wind-fixed coordinate system (X, Y) allows simplification of the basic equations of motion to

$$\dot{P} = -u \cos\beta_2 \quad (19)$$

$$P \dot{\theta} = -u \sin\beta_2 \quad (20)$$

$$\dot{\psi} = \dot{\theta}_2 + \dot{\beta}_2 \quad (21)$$

with the resulting control function independent of wind speed. In all cases the target is assumed to be the origin of inertial axes (x, y) .

3.0 An Application of Optimal Control Theory*

In this section the control of a gliding airdrop system is viewed in the context of optimal control theory. The basic philosophy is taken that at sometime t_0

*Acknowledgement - Appreciation is extended to Dr. Krister Martensson of Lund Univ for providing the computer program for obtaining trajectories, and to Mr. Kuang-Chung Wei of Brown Univ for computational assistance.

intermediate between the launch time 0 and the terminal T an estimate of the wind vector is made available based on measurements taken in the interval $0 \leq t \leq t_0$. Under the assumption that the wind remains constant over $t_0 \leq t \leq T$, an optimal control problem is formulated which minimizes the terminal distance error from the target. The filtering problem of estimating the wind based on available measurements is not considered in this paper.

Assuming a constant wind in the horizontal plane with components (W_x, W_y) and a constant rate of descent, the equations of motion governing the parachute in cartesian coordinates are given by

$$\dot{X} = u \cos\gamma + W_x \quad (22)$$

$$\dot{Y} = u \sin\gamma + W_y \quad (23)$$

$$\dot{\psi} = \frac{g}{u} \tan\phi \quad (24)$$

where \vec{u} is the velocity vector of the parachute relative to air with components $u_x = u \cos\omega$ and $u_y = u \sin\omega$, and ϕ is the bank angle of the parachute. The magnitude of \vec{u} , $u = (|u_x|^2 + |u_y|^2)^{1/2}$, is assumed to be constant and hence control is exerted through by rotations in the servo-motor connecting the control lines.

Let a time-varying transformation of the origin be made according to

$$X = x + (T-t)W_x \quad (25)$$

$$Y = y + (T-t)W_y \quad (26)$$

Then minimizing the terminal distance $p(T) = [|x(T)|^2 + |y(T)|^2]^{1/2}$ is equivalent to minimizing $[|X(T)|^2 + |Y(T)|^2]^{1/2}$. In addition let the independent variable be transformed via

$$\tau = \frac{t - t_0}{T - t_0} \quad (27)$$

and define new dependent variables via

$$X_1 = \frac{X}{u(T-t_0)}, \quad Y_2 = \frac{Y}{u(T-t_0)}$$

$$X_3 = \gamma, \quad \mu = \frac{(T-t_0)g}{u} \tan\phi$$

In terms of these variables the equations of motion become

$$X_1' = \cos X_3 \quad (28)$$

$$X_2' = \sin X_3 \quad (0 \leq \tau \leq 1) \quad (29)$$

$$X_3' = \mu \quad (30)$$

where prime denotes differentiation with respect to τ .

The problem is to determine a control function $\mu(\tau)$, $0 \leq \tau \leq 1$, which minimizes the terminal distance from the target, $[X_1(1)^2 + X_2(1)^2]^{1/2}$, while not requiring excessively large bank angles. The following performance index reflects a number of desirable features for this problem.

$$2P = |X_1(1)|^2 + |X_2(1)|^2 + q_1 |X_3(1) - \omega - \pi|^2 + q_2 \int_0^1 \mu^2 d\tau \quad (31)$$

The first weighting parameter ($q_1 \geq 0$) reflects the desirability of having the parachute point upwind at the terminal time in order to reduce the total horizontal velocity at touch-down. The second parameter ($q_2 \geq 0$) weights the "cost" of control on the interval $0 \leq \tau \leq 1$ and guarantees a finite value to the quadratic content of the optimal control signal. Putting $q_1 = 0$, the problem can be formulated with the terminal constraint that $X_3(1) = \omega + \pi$. Putting $q_2 = 0$ requires a side constraint on μ such as $|\mu(\tau)| \leq M$, $0 \leq \tau \leq 1$, in order to have a meaningful problem.

In terms of optimal control theory (3), the Hamiltonian for the unconstrained problem ($q_2 > 0$, $M = \infty$) with the equations of motion as in Eq (28), (29), (30) is given by

$$H(\lambda, X, \mu) = \lambda_1 \cos X_3 + \lambda_2 \sin X_3 + \lambda_3 \mu + \frac{1}{2} q_2 \mu^2 \quad (32)$$

where $(\lambda_1, \lambda_2, \lambda_3)$ are the adjoint variables which satisfy the differential equations: $\lambda_i' = -\frac{\partial H}{\partial x_i}$, $i = 1, 2, 3$.

Applying the "Minimum Principle" of optimal control theory, the necessary conditions for Eq (31) to achieve a minimum are that $H(\lambda, x, \mu)$ be minimized over μ , i.e. $\mu = -\lambda_3 / q_3$, and that the following transversality conditions be satisfied.

$$\lambda_1(1) = X_1(1), \lambda_2(1) = X_2(1)$$

$$\lambda_3(1) = q_1 [X_3(1) - \omega - \pi]$$

(If $q_1 = 0$ the terminal constraint on λ_3 is replaced by the terminal constraint on X_3 : $X_3(1) = \omega + \pi$.)

Solutions to the above unconstrained optimal control problem have been obtained using an algorithm due to Martensson (4). Since the computations are carried out in the normalized coordinates, the resulting trajectories represent the solution to a continuum of initial data in the inertial coordinate system via the relations

$$X(t) = u [T-t_0] \left[X_1 \left(\frac{t-t_0}{T-t_0} \right) \right] - W_x [T-t] \quad (33)$$

$$Y(t) = u [T-t_0] \left[X_2 \left(\frac{t-t_0}{T-t_0} \right) \right] - W_y [T-t] \quad (34)$$

$$\psi(t) = X_3 \left(\frac{t-t_0}{T-t_0} \right) \quad (35)$$

$$\phi(t) = \tan^{-1} \left(\frac{u / g \mu \left(\frac{t-t_0}{T-t_0} \right)}{(T-t_0)} \right) \quad (36)$$

The corresponding trajectories in inertial coordinates are shown in Figure 2. Note that the variation in bank angle is the same for each of the two wind conditions (Figure 3).

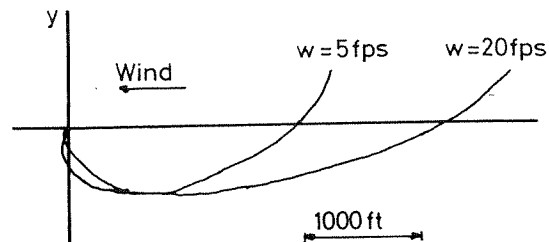


FIG 2 EXAMPLE OF OPTIMAL TRAJECTOR.

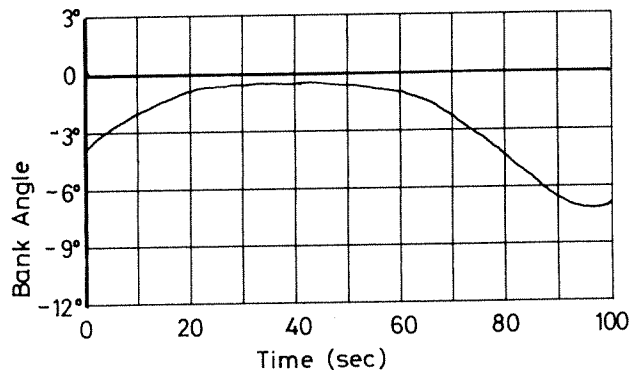


FIG 3 BANK ANGLE VARIATION FOR TYPICAL OPTIMAL TRAJECTORY

A study of the optimal trajectories is useful in establishing the region of initial conditions from which it is possible to reach the desired target. This region is contained within the unit circle in the normalized coordinate system. Further studies should reveal the degree to which reasonable terminal accuracy can be achieved under optimal control using a modest control deflection. However, such trajectories lend very little insight as to the nature of the optimal feedback control law. Essentially this involves obtaining a closed-form solution to the nonlinear two-point boundary value problem for arbitrary initial data. An initial study in obtaining this solution has been given, but more remains to be accomplished before substantive results can be reported of any practical utility. (5)

4.0 Solutions of Equations of Motion

4.1 Deployment Window

The simplest solution to the equations of motion is for the case of straight flight in uniform wind. This solution yields an important result which may be used to define the suitable region for initial deployment (i.e., "deployment window") for all sophisticated control functions. The locus of initial positions from which a straight path to the target can be flown in time $T = h/v$ is given by the equation

$$(x + W_x h/v)^2 + (y + W_y h/v)^2 = (u h/v)^2 \quad (37)$$

which at a particular altitude h is a circle of radius $(u h/v)$ centered upwind at the point $x = W_x h/v$, $y = W_y h/v$. Straight flight is accomplished by maintaining a heading toward the center of the circle. Note that if, at one level, flight is initiated at the edge of the circle with proper heading, the relative position on the circle will remain at all subsequent levels. The target (i.e. - the origin) is within the circle as long as $u > w$. The key feature of this circle is that it represents the absolute limit of deployment positions at a given altitude from which the target can be reached for a given average wind vector. If a glider is deployed outside the circle it cannot possibly reach the target maintaining velocity components u and v . But if it is deployed inside the circle it has excess time during which it can maneuver. However, if it is inside and near the edge of the circle but is not headed toward the center, then it also may not reach the target because of altitude lost during the required turn. The direct proportionality to altitude may be used to compensate for heading error by calculating the circle dimensions for an altitude higher than the actual deployment altitude according to the altitude lost during a 180 degree turn. Simulation of manual control has demonstrated that the entire area within the compensated circle is usable for deployment. The derivation of the circle remains valid for the average or height-integrated wind vector in a varying wind.

Automatic homing methods may not be able to use the entire deployment circle because of certain characteristics peculiar to the guidance mathematics. For example, radial homing (Section 4.2) requires a deployment window which is an ellipse whose major axis coincides with the diameter of the circle along the wind direction and whose minor axis is equal to

$$\sqrt{u^2 - w^2} (h/v)$$

This may be considered indicative of the inefficiency of radial homing in high winds. (Figure 4) A more sophisticated control method such as Method D discussed in Section 4.3 and 5.0 may use the entire

circle as a deployment window. For varying winds a deployment window may be constructed using the circle (or the ellipse) although some altitude compensation should be allowed. Assume ranges of $W_1 \leq W \leq W_2$ and $\omega_1 \leq \omega \leq \omega_2$ for the magnitude and direction respectively, of the wind and then construct circles (or ellipses) for each of the four cases (W_1, ω_1) , (W_1, ω_2) , (W_2, ω_1) and (W_2, ω_2) . The deployment window is then the common intersection of the four regions (Figure 5).

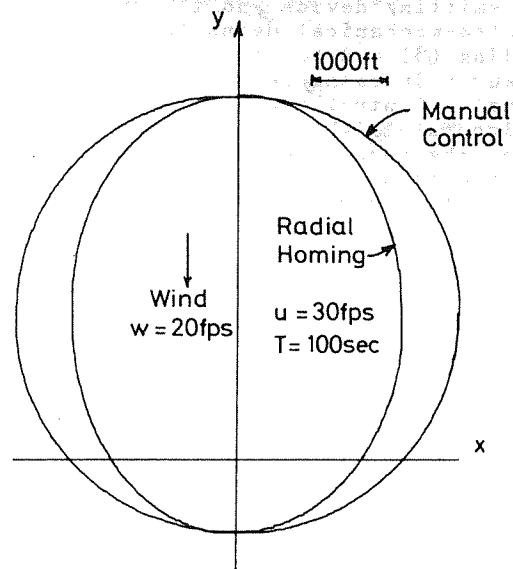


FIG 4 DEPLOYMENT WINDOW FOR UNIFORM WIND

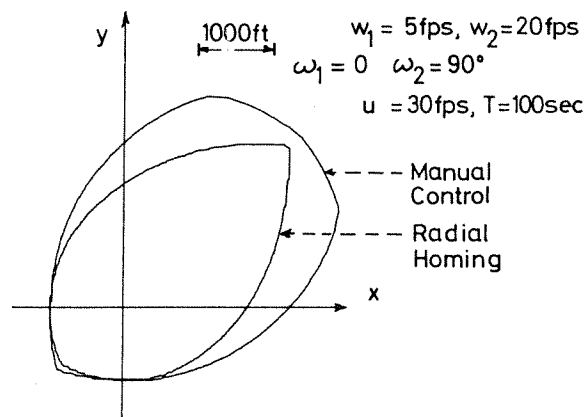


FIG 5 DEPLOYMENT WINDOW FOR VARIABLE WIND

At a given altitude, the size of the deployment window is proportional to the glide ratio (u/v) . For glide ratios of 3 or greater the deployment windows above 1,000 ft. become significantly large. A size can be chosen which would allow a particular transport aircraft to circle within the deployment window thereby removing the dependency of accuracy on exit interval. This feature of the deployment window is a clear indication of the superiority of gliding airdrop systems over

standard airdrop systems in that, for comparable accuracy, the deployment window for standard airdrop systems is merely a point!

4.2 Radial Homing

Radial homing is very attractive from the view point of minimizing the amount and sophistication of peripheral equipment. Typically the elements of a radial homing system would consist of a signal transmitting device and the appropriate electro-mechanical means to sense relative heading (β) and to cause the parachute to maneuver in response to the transmitted signal. Control over the direction of the horizontal flight path is thus effected by using the ground to air communication to fix the angular orientation between the parachute's airspeed vector and the transmitter.

Radial homing is defined in the strict sense by direct constant alignment of the parachute's airspeed vector with a radial line from the intended target.⁽⁶⁾ With no disturbing wind this steering routine would produce a straight line course to the target. Practically, however, wind effects must be reckoned with to determine trajectory characteristics and launch criteria. Under the assumption of a uniform wind velocity and constant gliding airspeed the two single differential equations which embody the kinematics of radial homing are Eq's (1) and (2) with $w_y \hat{=} w$, $w_x \hat{=} 0$ and $\beta \hat{=} 0$. Closed form solutions to this set are obtainable by direct integration giving the relationships

$$r = K \sec \theta (\sec \theta + \tan \theta)^\lambda \quad (38)$$

$$ut/P_0 = (\lambda/\{\lambda^2 - 1\})(\lambda - \sin \theta_0) \quad (39)$$

Where:

(1) K is a constant of integration dependent upon deployment conditions.

(2) $\lambda \hat{=} u/w$, the wind penetration parameter.

(3) $(\)_0$ denotes launch value. Eq (39) is carried out between the limits of P_0, θ_0 to the position where P is zero, so that t represents the total time to reach the target from a variety of launch positions.

The trajectory relationships Eq (38) shows that under the radial guidance constraint, a gliding system without wind penetration ability (i.e. $\lambda \leq 1$), can never pass directly over the intended point of impact. However, when the glide airspeed is greater than the wind speed ($\lambda > 1$) the parachute has the potential of always reaching the target, provided there is sufficient flight time. Eq (39) defines the flight time for any specified radial

coordinate selected relative to the target and a longitudinal axis aligned into the wind. When the time is fixed Eq (29) can be written in the form

$$P_0 = J / \{1 - (1/\lambda) \sin \theta_0\} \quad (40)$$

where

$$J = (ut)(\lambda^2 - 1)/\lambda^2 \text{ is a constant.}$$

This equation is the polar form of an ellipse and represents the region in which a radial homing trajectory will generally have sufficient altitude to fly over the target prior to impact (Section 4.1).

Eq's (38) and (39) describe the performance of the radial homing steering law neglecting variable wind and finite radius of turn effects. The general target-seeking attributes implied by Eq's (1) and (2) and embodied in Eq (38) are relatively unaffected by the idealizations assumed herein. In practical applications, the accuracy of radial homing is largely determined by the character of the orbit flown after reaching the vicinity of the target by a system having a finite radius of turn. A discussion of this aspect has been previously reported.⁽¹⁾⁽²⁾ The motion of the system after reaching the target is governed by the equations

$$X = r [1 + \cos(ut/r)] \quad (41)$$

$$Y = -r[(ut/r\lambda) - \sin(ut/r)] \quad (42)$$

for $0 \leq (ut/r) \leq 2\pi$. This motion consists of a 360 degree rotation from a position over the target (heading upwind) to a position downwind of the target from which straight homing flight back to the target is executed. Since, in general, such uncontrolled variables as exact position within the deployment window and initial heading will cause variation in the altitude at which radial homing to the target is completed, it is reasonable to assume that the probability of landing position and orientation is proportional to the time spent on various portions of the orbit. Position probability has thus been found to vary according to the following relation (Figure 6)⁽¹⁾

$$R_c/r = \frac{1.70 - 0.84 w/u}{1.27 - w/u} \quad (43)$$

The probability of landing at a speed less than u is given by Figure 7.

$$p = \left(\frac{1+w/u}{2}\right) - (1-w/u) \frac{\arcsin(w/u)}{\pi} \quad (44)$$

Eq (43) is derived from the ratio of time spent facing upwind (between the extreme points of the orbit) to the total orbit time.⁽¹⁾

4.3 Perfect Uniform-Wind Trajectory

After some examination of the basic equations of motion (Section 2.3) it

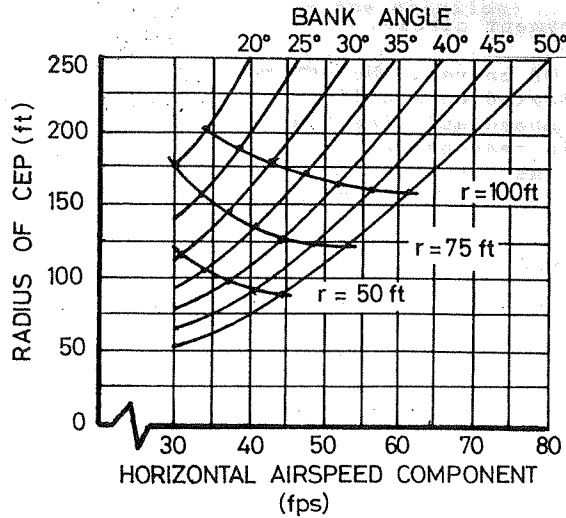


FIG 6 PREDICTED ACCURACY OF RADIAL HOMING (BANG-BANG) IN 25 FPS WIND

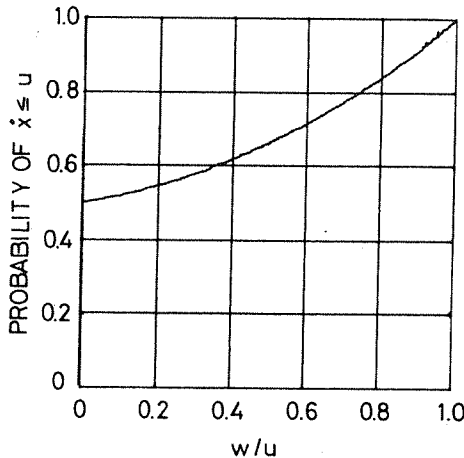


FIG 7 PROBABILITY OF $\bar{x} \leq u$ vs WIND SPEED RATIO w/u FOR RADIAL HOMING

becomes apparent that both the problem of miss-distance and of orientation into the wind at landing could be solved by employing the control law

$$\beta = \theta/k \quad (45)$$

where k would have some constant value. This law restrains β to approach zero as θ approaches zero. Thus, if the axis from which θ is measured is defined to point downwind, and if some reasonable function permits variation of altitude such that altitude approaches zero as β approaches zero the problem could be solved. Substitution of Eq (45) into the basic equations of motion (Eq's (19) and (20)) yields

$$\dot{p} = -u \cos(\theta/k) \quad (46)$$

$$p \dot{\theta} = -u \sin(\theta/k) \quad (47)$$

from which it follows that

$$(1/p)dp = \cot(\theta/k) d\theta \quad (48)$$

This may be integrated to obtain the ground track

$$\frac{p}{p_0} = \left(\frac{|\sin(\theta/k)|}{|\sin(\theta_0/k)|} \right)^k \quad (49)$$

in which the subscript () denotes initial conditions. Eq (48) allows a substitution for p in Eq (46) to obtain

$$dt = \frac{-p_0}{u} \left(\frac{\sin(\theta/k)}{\sin(\theta_0/k)} \right)^{k-1} d\theta \quad (50)$$

or

$$T = \left(\frac{p_0}{u} \left[\frac{\sin(\theta_0/k)}{\sin(\theta/k)} \right]^k \right) \int_0^{\theta_0} [\sin(\theta/k)]^{k-1} d\theta \quad (51)$$

For various integral values of k , complete solutions can be obtained for both the trajectory and for the required flight time T to the target from any initial point (p, θ) . Also we can convert T to altitude h_c by the simple relation $h_c = vT$ so that at any point (p, θ) an altitude h_c can be computed from which flight to the target can be made using the law $\beta = \theta/k$.

After examination of the properties of Eq's (49) and (51) it is apparent that for $K = 3$ a suitable steering rationale can be formulated using r/u as the control parameter

$$\frac{r}{u} = \frac{a}{180 \left(\frac{|\theta|}{540} \right) (h_c/h)^n} - \beta \quad (52)$$

where

$$h_c = \frac{3p v/u}{\sin^3(\theta/3)} \left(\frac{\pi \theta}{6(180)} - \frac{\sin(2\theta/3)}{4} \right) \quad (53)$$

Eq (52) is a feedback steering law which tends to drive β toward $\theta/3$ for $h_c = h$, to drive β toward 180 degrees for $h_c > h$, and to drive β toward zero for $h_c < h$. The underlying rationale is that while motion is generally toward decreasing θ , at any value of θ , h_c increases as p increases so that if too close and too high the corrective action is to fly radially outward (Figure 8). Eq (52) can be modified to limit the minimum turn radius

$$\frac{r}{u} = \left[\frac{a}{180 \left(\frac{|\theta|}{540} \right) (h_c/h)^n} - \beta \right] + \frac{r}{u} \min \quad (54)$$

The parameter n may be varied to control the abruptness with which steering goes from $\theta/3$ to zero or to 180 degrees. A value of $n = 20$ gives a virtual step function. Values in the range $2 \leq n \leq 10$ tend to give the best results.

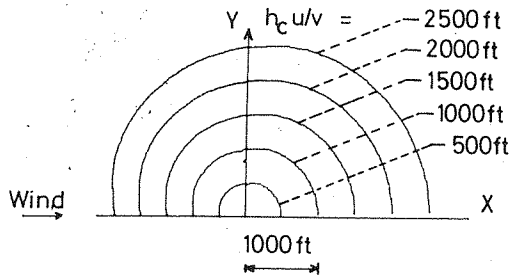


FIG 8 CONSTANT h_c CONTOURS FOR METHOD D

Although the steering is not precise, the function is highly stable and results in excellent accuracy (Method D, Figure 9).

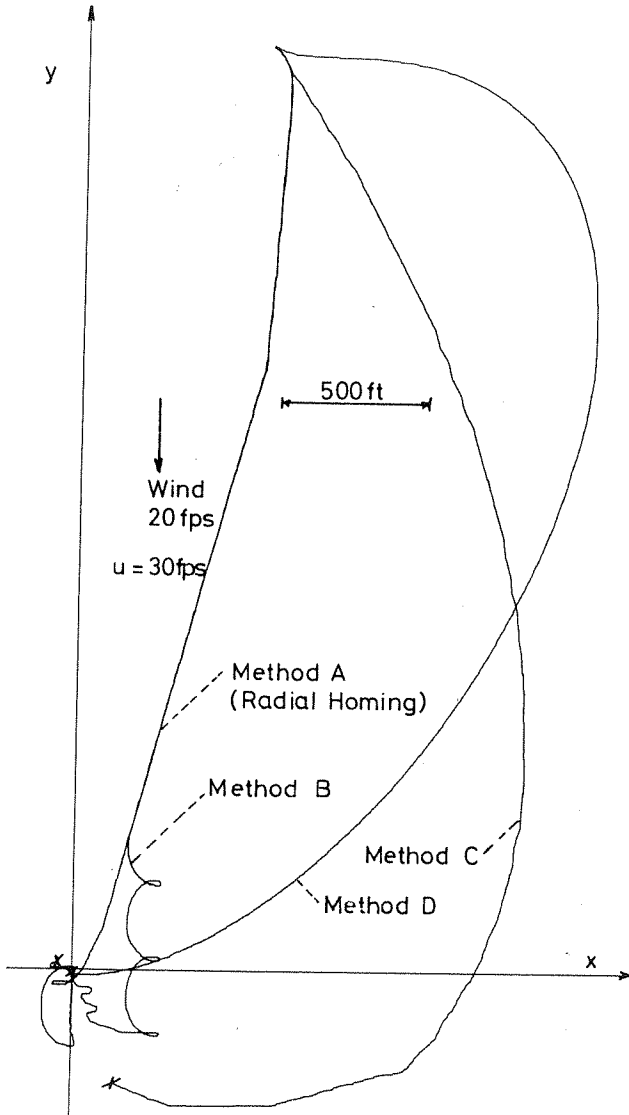


FIG 9 SAMPLE OF HOMING METHODS

If θ , p and β are relative to the wind fixed axes X, Y which are rotated so that X is parallel to the wind vector, nearly perfect accuracy and orientation is achieved (with no limitation on the wind speed) from any position ($p > 0$) within the appropriate

deployment circle.

Of course, the entire derivation is predicated on a uniform wind invariant in both speed and direction. In order to attain reasonable performance in varying winds as discussed in Section 5.0 the ratio h_c/h is multiplied by the factor

$$1 - b \frac{\Delta w}{\Delta t} \left(1 - \frac{|\theta|}{90}\right)$$

which appropriately biases the steering to partially compensate for wind gradients according to the rationale:

$\Delta w/\Delta t$	$ \theta $	h_c	β
< 0	< 90	increase	toward 180
< 0	> 90	decrease	toward 0
> 0	< 90	decrease	toward 0
> 0	> 90	increase	toward 180

A systematic method for determining appropriate values of b has not been formulated.

4.4 Other Homing Methods

Examination of Eq's (19), (20) and (21) shows several other possible "ad hoc" control methods. Two such methods are found by employing the relations $\dot{\beta} = K \sin \beta$ and $\dot{\beta} = K$. In each case, equations can be found for K such that p becomes zero at $t = T = h/v$. However, these functions do not allow control of orientation relative to the wind at landing.

5.0 Simulated Performance Study

5.1 Control Methods

Four automatic control methods were selected for comparative evaluation using computer simulation. These four methods represent a wide range of complexity and sophistication:

Method A - Non-proportional radial homing in which the glider turns with fixed angular increments and endeavors to point toward the target at all times. This is the simplest type of homing.

Method B - Radial homing with expanded cone of silence. This method is identical to Method A except that the cone of silence over the target is expanded so that its slope has approximately the same magnitude as the effective glide ratio of the glider. The glider is programmed to turn in a direction opposite to that in which it was turning upon entering the cone of silence and to maintain the turn until out of the cone of silence.

Method C - Modified conical homing in which range altitude and range-rate are sensed in addition to relative bearing with control to maintain a constant equality between range/altitude ratio and range-rate/rate of descent ratio. The glider flies along the surface of a cone whose vertex lies at the target. A modification

is added according to the equation:

$$\dot{\frac{P}{H}} = \frac{P}{h} + \left\{ K |\cos \beta| \frac{\dot{P}}{u} - 1 \right\} \quad (55)$$

which facilitates wind compensation to some extent.

Method D - Computed homing using Eq's (53) and (54) with Eq (54) modified for wind compensation (Section 4.3). This method is fully described in Section 4.3. It is the most sophisticated method requiring periodic measurement of range, azimuth, range-rate, azimuth-rate and altitude.

For general comparison, simulated manual control is used (Method E) as a performance baseline. This simulation incorporates real-time display of ground track with digital display of altitude, bearing and azimuth. The operator presses a key for left turn, right turn, or straight flight each second using his judgment of apparent closure rate. The operator is experienced and aware of the salient characteristics of each wind profile.

Figure 9 illustrates the performance of the automatic control methods in a uniform wind. For each flight airspeed is 30 fps, duration is 100 sec, maximum turn rate 35.5 degrees/sec as in all flights for this study. For illustration a 20 fps steady wind is used. The flight for Method A illustrates the typical approach and orbit as discussed in Section 4.2. The flight for Method B shows the typical effect of the cone of silence which usually causes a final approach into the wind though not always with such good accuracy (4 ft). The flight for Method C is a typical pattern although the poor accuracy is not typical. The flight for Method D illustrates the typically good performance in a uniform wind of any magnitude with gradual turns throughout (Accuracy: 8 ft).

Several control methods have been studied which are not presented in this paper since their performance was not comparable to that presented in this section. Proportional turn control for radial homing will not increase the accuracy although glide effectiveness might be increased. Several methods were studied which give excellent accuracy in uniform wind with random landing orientation. An attempt was made to achieve some degree of orientation by use of an initial aiming point downwind of the target. However, results were poor due to the wide variation in heading on arrival at the initial aiming point.

5.2 Wind Profiles

The parameters for the wind profiles are shown in Table 1. Profiles a through e were chosen as extreme cases in which

significant changes both in magnitude and direction occur although wind component accelerations are less than two ft/sec/sec. Profiles f and h have direction changes of less than 45 degrees over 100 sec and gradual decay in magnitude. Profile g has uniform direction with decaying magnitude. While no attempt has been made to simulate measured wind data, the wind profiles are indicative of extreme wind conditions as may be found in gusty winds over adverse terrain. The intent is to show performance in adverse conditions. Performance in more commonly encountered conditions is assumed to be better. A contracted study is currently being made by NLABS to study high wind environments and effects on aerial delivery systems from which more accurate wind profiles will become available.

5.3 Simulation Techniques

For the comparative performance study, the same airspeed (30 fps), duration (100 sec) and maximum turn rate (35.5 degrees/sec) were used in all cases. In Wind Profiles a through e, ten flights in each were made with each control method. Fifteen flights each were made in Wind Profiles f and h with twenty flights made in Wind Profile g. For each wind profile the same set of initial positions and orientations was used with each control method. For Methods C and D the modifying parameters were selected by trial and error for each wind profile but were held constant for all flights in a given wind profile.

5.4 Results

A summary of average miss distance and ground speed is shown in Table 2. The dimensionless ground speed is defined as

$$\dot{X} = \frac{\dot{X} - (u-w)}{2w} \quad (56)$$

which yields a value equal to 0 if directly upwind; equal to 1 if directly downwind; and equal to 0.5 if the speed equals the airspeed, u . Use of this parameter facilitates comparison of ground speed in the different winds. Analysis of the performance for Wind Profiles a through e shows that Methods B and C do not exhibit clear and consistent improvement over Method A. Therefore, only Methods A, D and E were studied in Wind Profiles f, g and h.

The overall average values are:

Miss-Distance (Wind Profiles a-e)	Std Dev	Dimensionless Groundspeed
Method A: 66 ft.	47 ft.	0.31
Method B: 61 ft.	44 ft.	0.21
Method C: 80 ft.	66 ft.	0.37
Method D: 66 ft.	65 ft.	0.45
Method E: 42 ft.	40 ft.	0.08

TABLE 1 WIND PROFILE CHARACTERISTICS

$$w_x = a_x \sin(b_x h + c_x), w_y = a_y \sin(b_y h + c_y)$$

$$(h_0 = 500 \text{ ft}, \dot{h} = -5 \text{ fps})$$

Profile	a_x	b_x	c_x	a_y	b_y	c_y	$W_x^*(0)$	$W_y^*(0)$	\bar{W}_x^*	\bar{W}_y^*	$W_x^*(H)$	$W_y^*(H)$
a	30	0.18	0	10	0.72	90	0	10	19	0	30	10
b	10	0.60	-60	20	1.20	-120	-9	-17	2	0	-9	17
c	15	0.18	-36	25	0.20	-40	-9	-16	2	4	12	22
d	20	0.10	-20	10	1.50	-300	-7	9	2	0	10	10
e	15	0.18	-36	25	0.50	-100	-9	-25	2	4	12	12
f	30	0.14	19.5	20	0.12	90	10	20	23	16	30	10
g	25	0.13	23.6	0	0	0	10	0	20	0	25	0
h	20	0.12	30	20	0.18	0	10	0	17	13	20	20

*Rounded to ft/sec

Miss-Distance
(Wind Profiles a-h)

Dimensionless
Groundspeed

Method A: 77 ft. 0.29
Method D: 66 ft. 0.37
Method E: 39 ft. 0.08

Histograms of the distribution of miss distance for Wind Profiles a through e are shown in Figure 10. The interval on the histograms is half the standard deviation centered on the mean value. In most cases the distributions are reasonable and detailed examination of the raw data indicates the variations are due to errors which may be considered random in nature. However, certain peculiarities were observed in the performance of Method D which indicate the deficiency of any control function which is derived in wind-fixed coordinates but which is forced to operate in varying winds. The individual flight performance in Wind Profiles b and c for Method D is shown below:

In Profile b, a peculiar condition was encountered in Run 86. The miss distance of 1,097 ft. is so far out that it unduly biases the data changing the average for Profile b from 125 ft. to 222 ft. and the average of 50 runs from 66 ft. to 86 ft. (changing the standard deviation from 65 ft. to 160 ft.). It was discarded in the data of Table 2. In Profile c, the average is 21 ft excluding

TABLE 3 SAMPLE CASES OF METHOD D

Run	X_0 (ft)	Y_0 (ft)	P (ft)	\dot{X} fps	
b	80	-500	200	39	29
	81	600	400	172	46
	82	-1000	-500	19	18
	83	-2000	-200	68	28
	84	2000	500	180	44
	85	2000	800	266	47
	86	500	2000	1097	48
	87	-2500	600	95	29
	88	-1500	1500	251	38
	89	-2000	-800	37	21
c	130	900	450	18	25
	131	1500	-500	22	30
	132	2000	1000	26	31
	133	1500	1500	27	35
	134	-1500	-104	23	31
	135	-2000	1500	21	23
	136	-2500	-800	20	19
	137	-1500	-2000	270	15
	138	500	-2500	16	19
	139	2000	-1500	12	20

Run 137. However, including Run 137 the average is 46 ft. Both Run 86 and Run 137 are peculiar cases where the control function was badly "fooled" by the wind variation.

5.5 Conclusions

The observed improvement of the more sophisticated homing methods (B and D) over the simple method of radial homing is only

TABLE 2
Summary of Performance

Wind Profile	Control Method	Max Dist	Avg Dist	Max Spd	Avg Spd	Dim Avg Spd	
a	A	121	78	38.3	31.0	0.55	
	B	117	63	39.9	30.5	0.53	
	20.0 * 40.0	C	86	37	39.7	30.2	0.51
	D	96	41	40.0	24.4	0.22	
	E	152	64	22.6	20.9	0.05	
b	A	173	41	28.4	14.6	0.10	
	B	177	77	49.1	15.5	0.13	
	10.6 * 49.6	C	165	91	44.8	23.4	0.33
	D	266	125	47.8	34.8	0.62	
	E	152	54	22.4	13.6	0.08	
c	A	152	84	40.9	24.9	0.36	
	B	171	55	31.6	15.0	0.09	
	11.7 * 48.3	C	150	67	47.6	24.9	0.36
	D	270	46	34.6	24.9	0.36	
	E	121	36	18.0	14.4	0.07	
d	A	142	75	40.1	29.2	0.46	
	B	122	56	32.9	24.8	0.26	
	19.0 * 41.0	C	72	42	41.0	29.9	0.50
	D	186	65	38.4	27.7	0.40	
	E	86	33	32.0	21.7	0.12	
e	A	162	51	26.8	8.2	0.08	
	B	96	64	10.3	5.8	0.04	
	3.8 * 56.2	C	305	165	53.2	12.2	0.16
	D	97	58	53.1	36.7	0.63	
	E	97	24	24.6	7.8	0.08	
f	A	621	120	35.9	14.0	0.14	
	7.9 * 52.1	D	170	51	41.2	18.8	0.25
	E	157	49	15.7	11.9	0.09	
g	A	138	65	39.9	26.4	0.32	
	20.0 * 40.0	D	91	45	40.0	23.9	0.20
	E	126	33	27.9	21.6	0.08	
h	A	135	79	36.4	26.5	0.33	
	20.0 * 40.0	D	301	108	39.6	29.1	0.46
	E	62	28	23.4	20.7	0.04	

* minimum attainable ground speed, fps
maximum attainable ground speed, fps

slight. The numerical values of the average are perhaps not as significant as the distribution shown in Figure 10 which shows that the performance of Method A is least erratic. The intent of this study is merely to show the relative performance capability and not to predict the absolute performance of each of these control methods. However, it must also be considered that any system capable of an average miss distance of less than 100 ft. would be a substantial improvement over any existing aerial delivery system particularly considering the adverse wind conditions studied here. Unfortunately, time has not permitted study of the effects of varying airspeed and maximum turn rate which would change the absolute miss distances and which might also change the relative performance. In general, however, the performance would be proportional to the ratio of wind speed to airspeed.

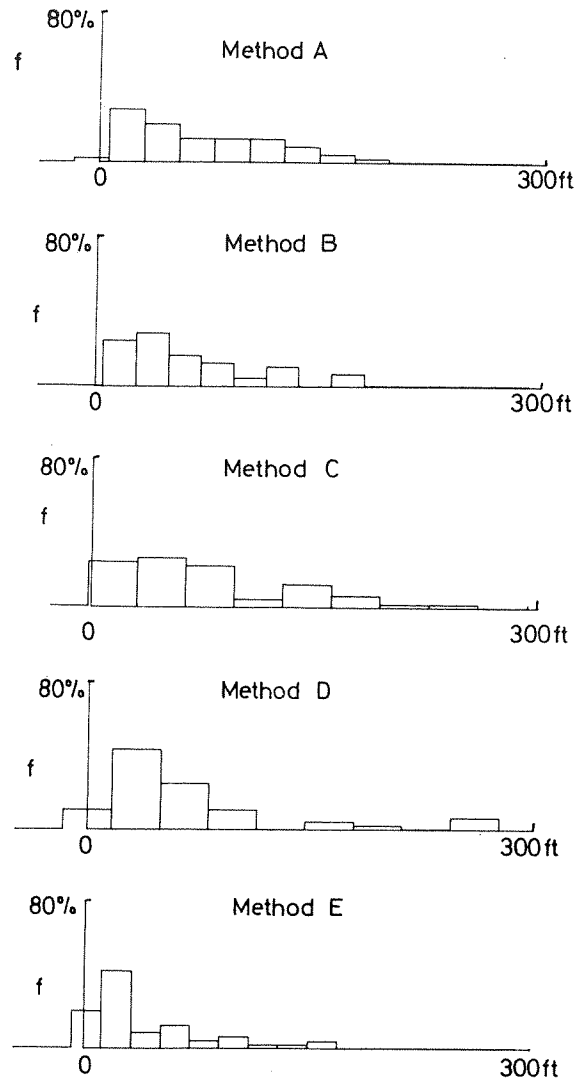


FIG 10 HISTOGRAMS OF MISS-DISTANCE

6.0 Summary

The analytical methods incorporating optimal control theory and the closed-form solution for the steering law $\beta = \theta/k$ appear to be the ultimate treatment of the problem under the uniform wind assumption. It is apparent, however, that significant improvement over the performance of simple radial homing in a realistic wind environment can only be realized if the problem is formulated for a stochastically varying wind. There may well be a feedback control law which will achieve better performance. Further work in this area may prove fruitful. For a suitable first generation of gliding airdrop systems, radial homing should be used with parameters selected for specific operational requirements.

References

1. Goodrick, T.F., "Wind Effect on Gliding Parachute Systems with Non-proportional Automatic Homing Control", TR 70-28-AD, US Army Natick Laboratories, 1969
2. Goodrick, T.F., "Estimation of Wind Effect on Gliding Parachute Cargo Systems Using Computer Simulation", AIAA Paper No. 70-1193, AIAA Aerodynamic Deceleration Systems Conference, 1970
3. Athans, M. and Falb, P., Optimal Control, McGraw-Hill Book Co., New York, 1966
4. Martensson, K., "New Approaches to the Numerical Solution of Optimal Control Problems", Report 7206, Lund Institute of Technology, 1972.
5. Pearson, A.E., "Optimal Control of a Gliding Parachute System", TR 73-30-AD, US Army Natick Laboratories, 1973
6. Murphy, A.L. Jr., "Trajectory Analysis of a Radial Homing Gliding Parachute in a Uniform Wind", TR 73-2-AD, US Army Natick Laboratories, 1971